Landscape Architecture

ARTICLE

Roof-to-Street Cooling and Day–Night Radiant Response around the Javits Green Roof during Hudson Yards High-Rise Completion

Kongjian Yu*

College of Architecture and Landscape Architecture, Peking University, Beijing 100871, China

* Correspondence: kjyu@urban.pku.edu.cn

Abstract

Green roofs with large areas can contribute towards reducing roof level temperatures, although their effectiveness in densely populated urban environments is conditional upon the extent to which this cooling is experienced at pedestrian height and influenced by nearby high-rises. This study evaluates the impact of the Jacob K. Javits Convention Center green roof and the adjacent Hudson Yards area in New York City for 2014, 2018, and 2021 urban geometries. The numerical framework consists of a 27 316 m^2 extensive green roof, a horizontal grid of 6 m by 6 m, vertical grid spacing of 2 m, building heights of 82 m and 740.08 m, and typical weather conditions. The maximum roof-level cooling decreases from 0.75 K in 2014 to 0.65 K in 2018 and 0.64 K in 2021, whereas the maximum pedestrian-level cooling reduces from 0.52 K to 0.45 K and 0.44 K. The transfer fraction of roof to street cooling stays almost the same at roughly 0.69, implying reduced cooling capacity without the disruption of vertical transport of thermal energy. Maximum median sky view factor is 0.184 for 2018 and 0.194 for 2021. For the 2021 form, the mean radiant temperature reduction during the day is estimated to be 1.65 °C, while the increase.

Keywords: green roof; urban microclimate; Hudson Yards; sky-view factor; mean radiant temperature; roof-to-street cooling; ENVI-met validation

1. Introduction

Urban heat exposure results from the interplay between atmospheric forcing, surface coverage, building height, street design, radiation balance, ventilation, and material heat storage. The large-scale urban heat island studies indicated the characteristic property of an urban environment that keeps the urban surface hotter than its rural surroundings. Yet the difference in thermal exposure within a city is significant even within short walking distance because of variation in orientation, wall height, roof covering, vegetation placement, and sky view factor [15, 19]. High-rises can further complicate the local radiative heat budget depending on the configuration of streets and their placement relative to each other [8, 16, 21]. This variability in heat exposure becomes increasingly pertinent in areas that have existing environmental infrastructure and experience additional growth.

The role of green roofs is in moderation of roof surface heat absorption, stormwater retention, habitat creation,

Received: 22 December 2023; Revised: 27 February 2024; Accepted: 27 March 2024; Published: 30 June 2024.

doi: 10.70517/la20241142-04

and reduction of building energy use [7, 9, 14]. Green roofs cool according to substrate depth, surface albedo, vegetation coverage, evapotranspiration rate, leaf area index, and surface moisture content [2, 17, 28]. The green roof reduces the temperature over the vegetated surface, but the pedestrian layer experiences less cooling because it is further removed from the roof in space and time due to building height, urban roughness, and canyon flow [2]. Moreover, a high-rise district does not allow combining roof and street in one thermal level.

In addition to their impact on air temperature, vegetation affects radiant exposure. Vegetation shading, humidity, and air movement depend on its placement at the ground level or on a roof, whereas roof vegetation influences only the roof energy budget and immediate air above the surface [5, 10]. Studies of the effect of green roofs, green walls, and outdoor comfort revealed that the most pronounced effect on pedestrians comes from changes in radiation and air movement at pedestrian height [2, 4, 23]. The contribution of an extensive roof garden to the cooling is possible in terms of the roof-to-street cooling transfer, but not necessarily in terms of the rooftop temperature itself.

Adding high-rise buildings creates another thermal pathway. The lower sky view factor can diminish solar exposure during the day, but can also keep the surfaces warm overnight through reduced longwave emission [11, 12, 16]. Mean radiant temperature is a highly sensitive metric of thermal comfort because it responds to solar access, sky view, radiation reflection, and surface temperature [23, 25]. Dense urban environment, as a consequence, shows low daytime MRT load but maintains high nighttime MRT because of reduced longwave emission. Air temperature and mean radiant temperature must be analyzed separately without simplification into one single parameter.

High-resolution urban microclimate models have sufficient spatial and vertical resolution to account for all thermal pathways described above. The ENVI-met software simulates processes of surface–plant–air energy exchanges, canyon air flow, plant effects on air properties, and conditions of thermal exposure at the pedestrian height [6, 20, 24]. However, the interpretation of the simulation results requires validation, especially of the air temperature. Even though high correlation coefficient between measured and modeled data indicates agreement, low absolute error can be masked by significant differences at the pedestrian height. The validation values must therefore be included in the model comparison.

For this particular comparison, there is a focused geographical area, namely the Jacob K. Javits Convention Center and the Hudson Yards high-rise neighborhood, with consistent meteorology forcing. In 2014, the green roof was in place and no nearby high-rises existed. In 2018, the Hudson Yards were partially completed and consisted of three fully constructed buildings, two unfinished buildings, and three unoccupied sites. In 2021, the high-rise form was fully completed and simulated in the modeling experiment [3]. With this temporal progression, we are able to trace the changes in cooling at rooftop, street level, sky view, and day and night MRT shift.

The question posed at the site scale is simple enough: Does the presence of Hudson Yards high-rises reduce the cooling at the roof height, decrease the relative roof-to-street transfer, or change the pattern of MRT cooling by shifting it from daytime shade to night-time radiant load increase? The answer is provided directly through the comparison of the existing Javits values: roof cooling of 0.75 K, 0.65 K, and 0.64 K; pedestrian cooling of 0.52 K, 0.45 K, and 0.44 K; normalized median sky view factor values of 1.000, 0.816, and 0.806; daytime MRT shifts of 0.00, -0.14 °C, and -1.65 °C; midnight MRT shifts of 0.00, +0.65 °C, and +0.74 °C; and validation weights based on three receiver locations.

2. Javits–Hudson Yards Numerical Basis

2.1. Site Geometry and Receptor Locations

This study focuses on the intersection of the Jacob K. Javits Convention Center and the Hudson Yards high-rise area in Manhattan, NYC. The Javits Convention Center is characterized by a single rooftop area split into the north and the south roof segments by a middle section. Three receiver positions correspond to north and south roof surfaces and the pedestrian path along 11th Avenue.

The receptor set up in Figure 1 is the basis for this analysis. The roof cooling positions represent the validation of the vegetated roof, while the position along 11th Avenue represents the pedestrian level. In terms of vertical context,

the change is represented by comparing the 82 m 2014 domain height with the 740.08 m 2018/2021 domain height. This is due to the construction of Hudson Yards Towers in the new models. The picture thus shows the physical levels where cooling and validation values can be analyzed.

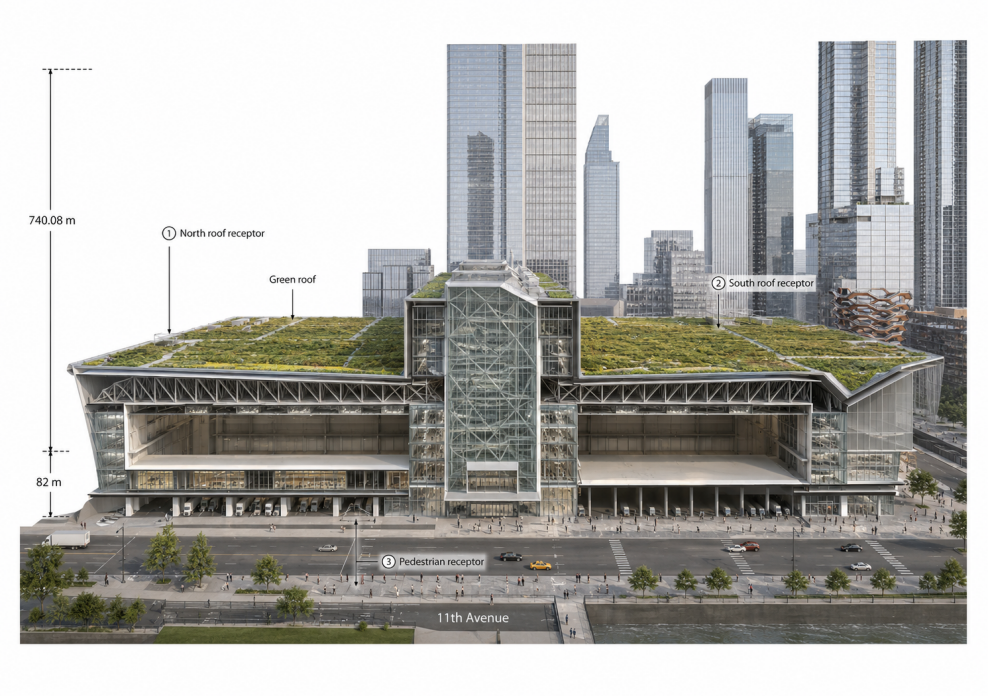

Figure 1. Javits roof receptor layout.

2.2. Urban Form Over Time

Three urban forms have been analyzed. In the 2014 form, there was already the constructed green roof, while the domain height was lower at 82 m. In the 2018 form, there were three completed high-rise buildings, two unfinished high-rise buildings, three empty plots, and an increased domain height to 740.08 m. In the 2021 form, the same domain height was used, but there were four additional buildings representing high-rise enclosure of the area. These are chronological forms of the district at different times.

Figure 2 depicts three forms of urban areas at different times with the same roof. 2014 urban form includes roof cooling of 0.75 K, pedestrian cooling of 0.52 K, and median sky view of 1.000. The urban form in 2018 includes roof cooling of 0.65 K, pedestrian cooling of 0.45 K, and median sky view of 0.816. The urban form in 2021 includes roof cooling of 0.64 K, pedestrian cooling of 0.44 K, and median sky view of 0.806.

2.3. Forcing, Cooling, and Sky-View Values

The calculation uses the same meteorological forcing across the three urban forms. The horizontal grid is 6 m by 6 m, and the lower vertical grid is 2 m. Average wind direction is 183°, average wind speed is 1.81 m s^{-1}, air temperature spans 18.35 °C to 32.84 °C, and relative humidity spans 46.10% to 81.09%. Because these forcing values are held constant, the comparison centers on surrounding form rather than weather variation.

The values in Table 1 show parallel decline in roof and pedestrian cooling. Relative median SVF falls from 1.000 to 0.816 after the first major high-rise build-out and then to 0.806 after completion. The small additional SVF decrease from 2018 to 2021 contrasts with the much larger visual change in completed tower form, showing why the radiant response must be read from MRT values as well as from median sky view.

Figure 2. Urban form sequence.

Table 1. Urban-form cooling values.

Urban form	Physical condition	Domain height (m)	Roof cooling (K)	Pedestrian cooling (K)	Relative median SVF
2014	Green roof present; high-rise enclosure not represented around the site	82.00	0.75	0.52	1.000
2018	Three completed buildings, two partial buildings, and three empty lots	740.08	0.65	0.45	0.816
2021	Completed Hudson Yards high-rise form in the model domain	740.08	0.64	0.44	0.806

3. Thermal Calculations

3.1. Roof Cooling Retention and Morphology Attenuation

Let y denote the 2014, 2018, or 2021 urban form. Let C_y^R be maximum roof-level air-temperature cooling and C_y^P be maximum pedestrian-level air-temperature cooling. Both are positive cooling magnitudes in kelvin. Roof cooling retention is calculated as

$$\mathrm{RCR}_y = \frac{C_y^R}{C_{2014}^R}. \tag{1}$$

The 2021 value of 0.853 means that 85.3% of the 2014 maximum roof cooling remains after completion of surrounding high-rise form.

Morphology attenuation is calculated as

$$\mathrm{MAF}_y = 1 - \mathrm{RCR}_y. \tag{2}$$

The 2021 value of 0.147 means that maximum roof cooling is 14.7% lower than in 2014. The value expresses proportional loss in the Javits cooling record and is not an additional simulation.

3.2. Roof-to-Street Transfer

The roof-to-street transfer fraction is calculated as

$$\mathrm{PTF}_y = \frac{C_y^P}{C_y^R}. \tag{3}$$

This ratio compares maximum pedestrian cooling with maximum roof cooling in the same year. It is not an areal average and does not imply uniform cooling at every sidewalk point. Its role is to determine whether increasing enclosure changes the proportional delivery from the elevated roof layer to the pedestrian layer.

3.3. Sky-View Compression and Radiant Timing

Sky-view compression is calculated as

$$\mathrm{SVC}_y = 1 - \frac{\mathrm{SVF}_y}{\mathrm{SVF}_{2014}}. \tag{4}$$

The 2014 form has SVC = 0 because it provides the reference median SVF ratio. The 2018 and 2021 values quantify the proportional reduction in median visible sky associated with the high-rise forms.

Day–night radiant balance is calculated as

$$\mathrm{RIB}_y = \Delta MRT_y^N - |\Delta MRT_y^D|, \tag{5}$$

where ΔMRT_y^D is the daytime pedestrian mean radiant temperature shift relative to 2014 and ΔMRT_y^N is the midnight pedestrian mean radiant temperature shift relative to 2014. Positive RIB indicates that the midnight increase exceeds the daytime reduction. Negative RIB indicates that the daytime reduction exceeds the midnight increase.

The calculation plate in Figure 3 places the five year-specific values together. RCR declines from 1.000 to 0.867 and 0.853. MAF rises from 0.000 to 0.133 and 0.147. PTF remains tightly grouped at 0.693, 0.692, and 0.688. SVC rises to 0.184 and 0.194. RIB changes direction, from +0.51 °C in 2018 to -0.91 °C in 2021. This combination shows that high-rise completion changes air-temperature magnitude and radiant timing in different ways.

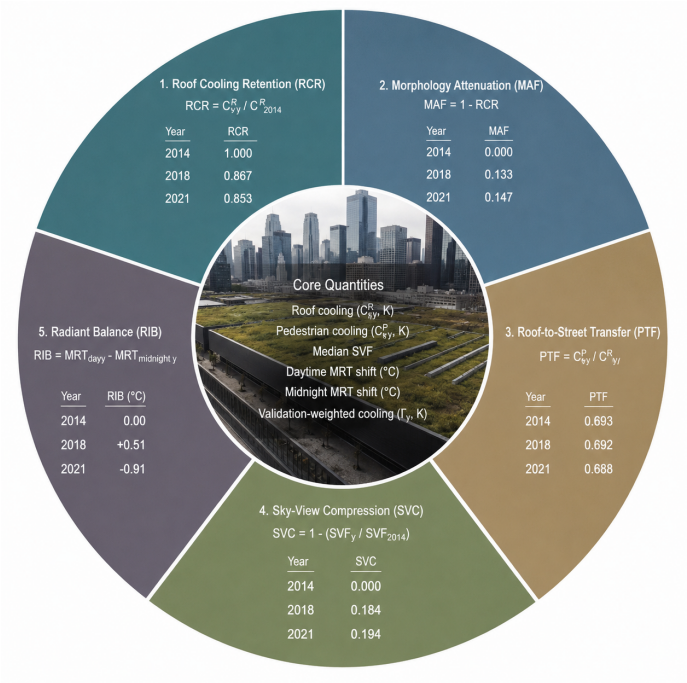

Figure 3. Thermal calculation values.

3.4. Validation Weighting

Air-temperature validation is incorporated through the coefficient of determination, root mean square error, and Willmott's agreement index [26]. For each receptor level z,

$$w_z = \frac{R_z^2 d_z}{1 + \mathrm{RMSE}_z}, \tag{6}$$

where R_z^2 is the coefficient of determination, d_z is Willmott's agreement index, and RMSE_z is in degrees Celsius. The equation assigns larger weights to receptor levels with high correlation, high agreement, and lower absolute error.

The roof weight is the average of the north and south roof weights. The pedestrian weight is calculated from the 11th Avenue validation values. Validation-weighted cooling is calculated as

$$\Gamma_y = \frac{w_R C_y^R + w_P C_y^P}{w_R + w_P}, \tag{7}$$

where w_R is the roof-average weight and w_P is the pedestrian weight. The result remains in kelvin and represents validation-weighted air-temperature cooling across roof and pedestrian levels.

4. Results

4.1. Receptor Validation

Air-temperature validation is strong at all three receptor positions, although the pedestrian receptor has the largest absolute error. The north green roof has $R^2 = 0.95$, RMSE of 0.66 °C, and $d = 0.98$, producing a weight of 0.561. The south green roof has $R^2 = 0.96$, RMSE of 0.71 °C, and $d = 0.98$, producing a weight of 0.550. The 11th Avenue pedestrian receptor has $R^2 = 0.96$, RMSE of 1.17 °C, and $d = 0.96$, producing a lower weight of 0.425.

The values in Table 2 justify the lower 11th Avenue weight without excluding the pedestrian receptor. Correlation and agreement remain high at the sidewalk, but RMSE is larger than at the roof. This difference is consistent with the greater small-scale variability of the pedestrian layer, where shade, reflected radiation, traffic-corridor openness, turbulence, and surface heterogeneity influence the local air temperature. The average roof weight is 0.556, while the pedestrian weight is 0.425.

Table 2. Air-temperature validation.

Location	R^2	RMSE (°C)	d	w_z
North green roof	0.95	0.66	0.98	0.561
South green roof	0.96	0.71	0.98	0.550
Pedestrian level at 11th Avenue	0.96	1.17	0.96	0.425

The validation graphic in Figure 4 shows why the weighted value remains closer to roof cooling than to pedestrian cooling. The roof receptors have similar weights, while the 11th Avenue value is reduced by its larger RMSE. The resulting Γ_y values are 0.650 K, 0.563 K, and 0.553 K. Street-level cooling remains included in every year, but it does not receive the same weight as the roof layer.

4.2. Cooling Magnitude and Vertical Transfer

Maximum roof-level cooling decreases from 0.75 K in 2014 to 0.65 K in 2018 and 0.64 K in 2021. Maximum pedestrian-level cooling decreases from 0.52 K to 0.45 K and 0.44 K. The absolute roof-level loss from 2014 to 2021 is 0.11 K; the absolute pedestrian-level loss is 0.08 K. These values indicate moderate attenuation rather than disappearance of the green-roof cooling signal.

The values in Table 3 identify the dominant air-temperature response. Roof cooling retention falls to 0.853 in 2021, but PTF remains between 0.688 and 0.693. The difference across the three PTF values is only 0.005. The completed high-rise form therefore weakens the cooling magnitude entering the vertical relationship; it does not create a sharp proportional loss between roof and sidewalk.

The paired trace in Figure 5 emphasizes the timing of the cooling loss. Roof cooling falls by 0.10 K from 2014 to 2018 and by only 0.01 K from 2018 to 2021. Pedestrian cooling follows the same pattern, falling by 0.07 K and then 0.01 K. Most air-temperature attenuation occurs during the initial transition to high-rise enclosure rather than during final completion.

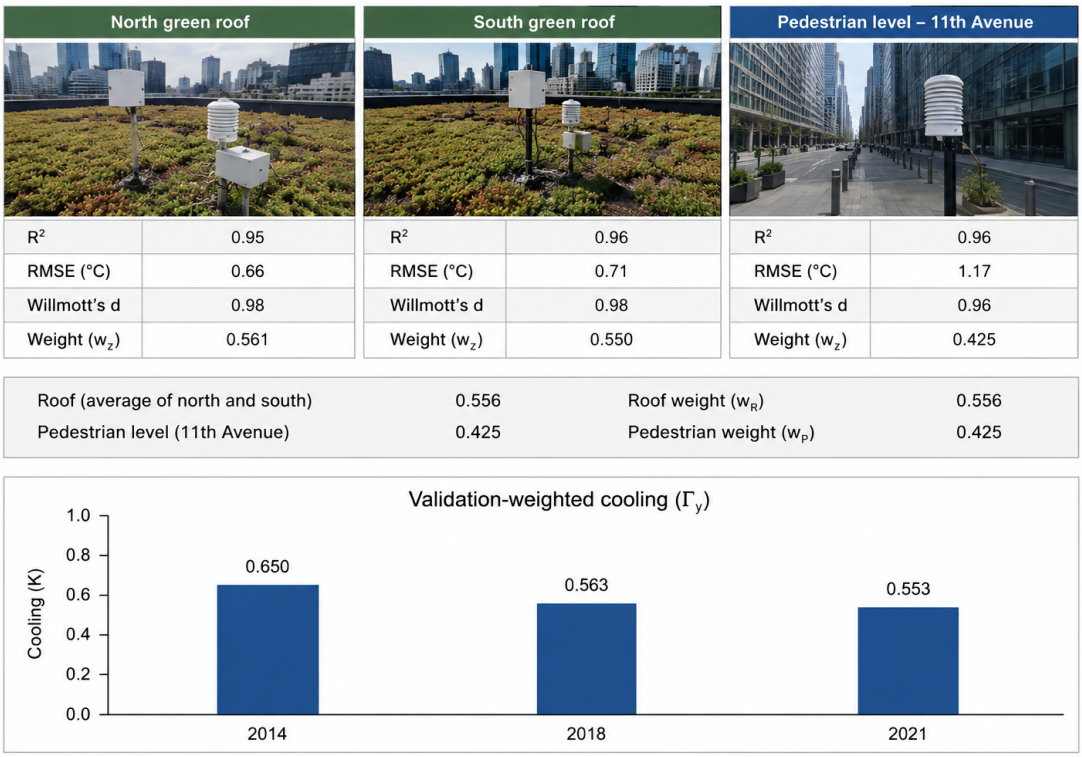

Figure 4. Validation-weighted cooling.

Table 3. Cooling and transfer values.

Urban form	C_y^R (K)	C_y^P (K)	RCR	MAF	PTF
2014	0.75	0.52	1.000	0.000	0.693
2018	0.65	0.45	0.867	0.133	0.692
2021	0.64	0.44	0.853	0.147	0.688

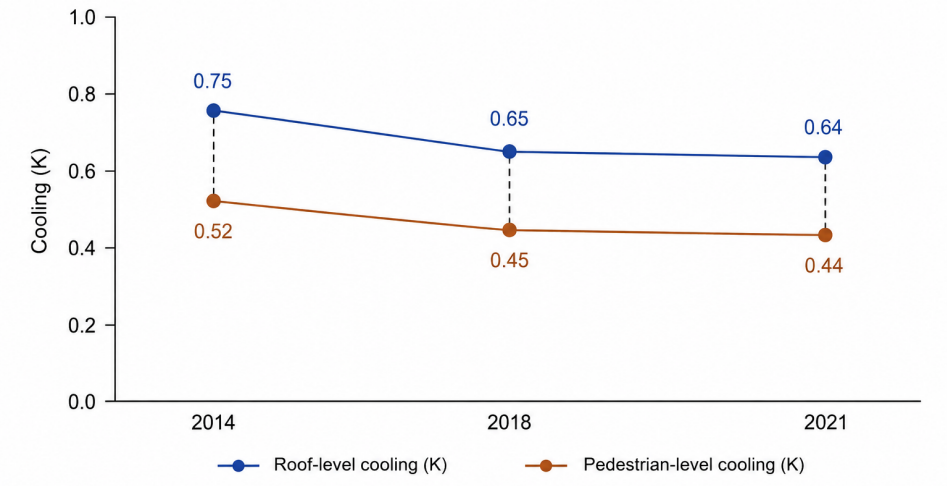

Roof-to-Street Transfer (PTF)	0.693	0.692	0.688

Figure 5. Roof and street cooling.

4.3. Sky-View Compression and Radiant Timing

Sky-view compression follows a different pattern from air-temperature cooling. Median SVC reaches 0.184 in 2018 and 0.194 in 2021, a difference of only 0.010 between the two high-rise forms. The daytime MRT response changes much more strongly: 2018 reduces daytime pedestrian MRT by 0.14 °C, while 2021 reduces it by 1.65 °C relative to 2014. The values in Table 4 show a clear day–night contrast. The 2018 form has RIB = +0.51 °C because the midnight increase of 0.65 °C exceeds the daytime reduction of 0.14 °C. The 2021 form has RIB = -0.91 °C because the daytime reduction of 1.65 °C exceeds the midnight increase of 0.74 °C. Completed high-rise enclosure therefore provides stronger daytime shade but still retains additional radiant warmth at midnight.

Table 4. Sky-view and MRT values.

Urban form	SVC	Daytime MRT shift (°C)	Midnight MRT shift (°C)	RIB (°C)
2014	0.000	0.00	0.00	0.00
2018	0.184	-0.14	+0.65	+0.51
2021	0.194	-1.65	+0.74	-0.91

The mirrored bars in Figure 6 make the radiant asymmetry visible. The 2018 condition is unfavorable in the selected day–midnight comparison because nighttime radiant increase is larger than daytime relief. The 2021 condition changes the balance through much stronger daytime shade. Median SVC alone cannot explain that shift because SVC differs only slightly between 2018 and 2021; tower placement, height distribution, and timing of shade must affect the daytime MRT value.

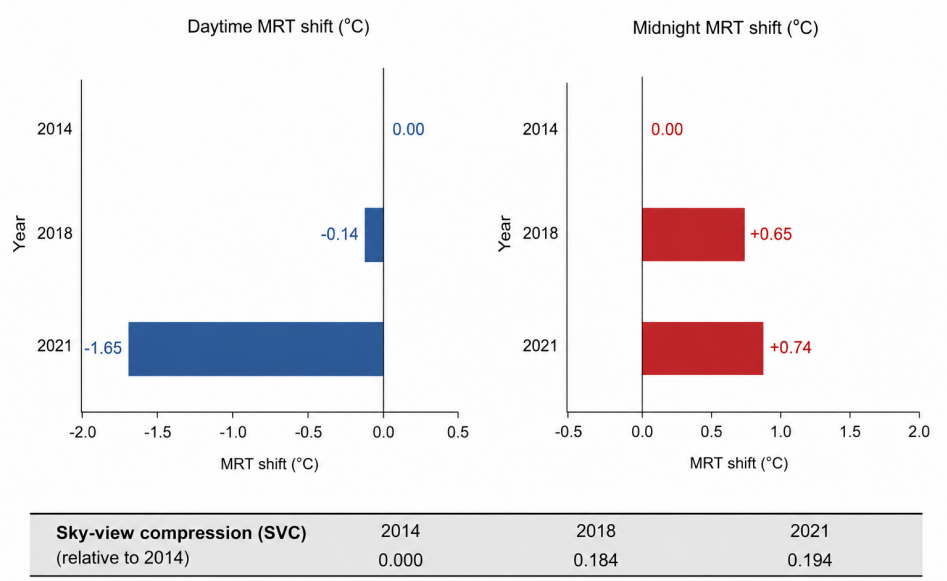

Figure 6. Day and midnight MRT.

4.4. Reliability-Weighted Cooling

Validation-weighted cooling declines from 0.650 K in 2014 to 0.563 K in 2018 and 0.553 K in 2021. The relative values are 1.000, 0.866, and 0.851. The completed high-rise form therefore retains 85.1% of the 2014 reliability-weighted air-temperature cooling value.

The values in Table 5 closely follow roof cooling retention because PTF is stable. The reduction from 2014 to 2018 is 0.087 K, while the reduction from 2018 to 2021 is 0.010 K. This pattern reinforces the result that air-temperature attenuation is concentrated in the first high-rise transition. The later 2018-to-2021 change alters radiant timing more strongly than maximum air-temperature cooling.

Table 5. Reliability-weighted cooling.

Urban form	Γ_y (K)	Relative Γ_y
2014	0.650	1.000
2018	0.563	0.866
2021	0.553	0.851

4.5. Thermal Outcomes by Design Target

The strongest urban form depends on the target thermal outcome. The 2014 form has the largest roof-zone cooling and pedestrian cooling. The 2021 form has the strongest daytime pedestrian MRT reduction. The 2014 form has the most favorable midnight radiant condition because both high-rise forms increase midnight MRT. Roof-to-street transfer is effectively stable across all three forms.

The target-specific reading in Table 6 prevents a single thermal label from overstating performance. A daytime pedestrian comfort target favors the 2021 shade effect. A midnight heat-release target favors the 2014 openness. A roof-management target favors the largest roof cooling value in 2014. The numerical contrast shows that roof greening and high-rise shade provide different thermal services.

Table 6. Strongest form by target.

Thermal target	Strongest form	Numerical interpretation
Maximum roof-zone air cooling	2014	Roof cooling is 0.75 K, compared with 0.65 K in 2018 and 0.64 K in 2021.
Pedestrian-level air cooling	2014	Pedestrian cooling is 0.52 K, compared with 0.45 K in 2018 and 0.44 K in 2021.
Roof-to-street transfer proportion	Similar in all forms	PTF remains between 0.688 and 0.693, indicating stable proportional delivery.
Daytime pedestrian radiant relief	2021	Daytime MRT is reduced by 1.65 °C relative to 2014.
Midnight radiant release	2014	The 2018 and 2021 forms increase midnight MRT by 0.65 °C and 0.74 °C.
Reliability-weighted cooling	2014	Γ_y is 0.650 K in 2014, 0.563 K in 2018, and 0.553 K in 2021.

Figure 7. Thermal target outcomes.

The portrait in Figure 7 separates the strongest outcome for each target. Air-temperature cooling belongs to 2014, daytime MRT relief belongs to 2021, and transfer proportion remains nearly unchanged. This separation supports

the numerical conclusion that high-rise enclosure modifies the balance among thermal services rather than making the green roof simply effective or ineffective.

The state map in Figure 8 combines relative validation-weighted cooling with RIB. The 2014 point is 1.000 and 0.00. The 2018 point moves to 0.866 and +0.51 °C, combining reduced cooling with a midnight-dominant radiant penalty. The 2021 point moves to 0.851 and -0.91 °C, combining slightly lower cooling with stronger daytime radiant relief. The movement from 2018 to 2021 is mainly a radiant shift rather than an air-temperature cooling shift.

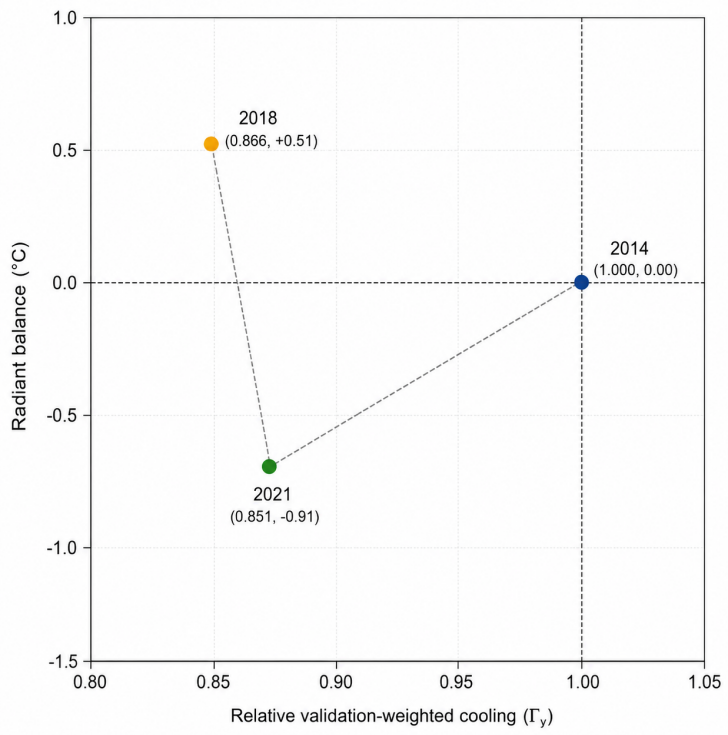

Figure 8. Cooling and radiant balance.

5. Discussion

5.1. Dominant Cooling Response

In accordance with this approach, cooling attenuation, rather than vertical disconnection, becomes the main air-temperature response in case of high-rise completion. The maximum roof-level cooling value will be 0.64 K, and the maximum pedestrian-level cooling value will be 0.44 K. The transfer fraction value stays between 0.688 and 0.693. This narrow range means that the ratio between the roof layer and street level stays consistent, whereas the amount of cooling conveyed through this ratio drops.

This change in the main response also impacts the overall meaning of design implications. A loss of proportionality in transfer from roofs to streets would imply insufficient vertical air-movement. In this context, the Javits–Hudson Yards comparison suggests preservation of roof cooling and introduction of pedestrian cooling elements. The latter could include shade provision on sidewalks, the use of cool pavement types, planting of street trees, and installation of materials limiting radiance.

The sequence of air-temperature responses is unique to the Javits case as well. The decrease in cooling from 2014 to 2018 makes up 0.10 K, whereas only 0.01 K cooling is lost between 2018 and 2021. The same goes for pedestrian cooling: the first major increase in surrounding buildings contributes more to cooling change than the last step in the transition process. It agrees with findings on vegetation-induced urban cooling driven by geometry, ventilation, and surface arrangement [2, 5, 10].

5.2. Daytime Cooling and Midnight Retention

The air-temperature cooling response and MRT shift are dissimilar in the case study. Whereas the difference in air-temperature cooling is not significant (0.75 and 0.64 °C for 2014 and 2021), respectively, daytime MRT difference rises from 0.14 °C to 1.65 °C. The roof cooling reduction in the period from 2018 to 2021 stands at 0.01 K. Hence, daytime cooling occurs through another pathway than maximum roof-level air-temperature cooling.

Mean radiant temperature depends on the solar angle and angular relationships among the sun, the sky, surfaces, and pedestrians. The small difference in median SVC may be coupled with large differences in daylight and midnight exposure of the pedestrian receptor due to the change in high-rise morphology. The new shape of buildings offers better pedestrian shading during the day, yet prevents midnight heat release. Such an outcome fits into the known characteristics of the urban canyon effect [8, 11, 16].

The 2018 intermediate shape turns out to be the least desirable choice from the standpoint of the radiant response. The difference in daytime MRT is just 8.5% of the 2021 difference, while midnight MRT increase is already 87.8%. As such, an extended development period causes many problems due to the intermediate form. Pedestrian shade, cool surfaces, and absence of waiting areas retaining midnight heat become critical issues.

5.3. Validation-Constrained Cooling Interpretation

The calculation of weighted cooling implies dependence on the degree of validation similarity. The higher reliability of roof-level predictions (RMSE values of 0.66 °C and 0.71 °C) results in a higher weight compared to the pedestrian layer (RMSE of 1.17 °C). The final Γ_y value is therefore not zero, but still lower than unweighted cooling values: it will decline from 0.650 K to 0.553 K and 0.563 K. Since the roof transfer proportion is consistent, the weighted result also stays close to the original.

The validity of the transfer value confirms the physical correctness of the weighted cooling sequence. If there were significant changes in proportionality, the cooling sequence might diverge from the original one significantly. Thus, the agreement between RCR, PTF, and Γ_y allows concluding that the main response lies in cooling magnitude and not proportionality.

Validation-based weighting does not turn Γ_y into a complete comfort index. There is no need to take into account humidity, pedestrian winds, human activity, and clothing for this particular task. Instead, the value reflects the validation similarity between the air temperatures measured on the roof and those experienced by pedestrians. MRT values should also be discussed separately due to their different purpose.

5.4. Design Implications for High-Rise Districts

Javits–Hudson Yards analysis highlights the multi-faceted nature of heat mitigation design. The presence of green roof allows maintaining the cooling effect on roof layer and producing an impact on pedestrian cooling. However, pedestrian exposure requires additional design solutions beyond roofs. The completed form shows how shading works, but also reveals the problem of heat retention. Designers should thus consider both cooling and radiant components of the problem.

Depending on the targeted area, the most optimal option varies considerably. Roof-zone cooling maximization suggests 2014 with 0.75 K of cooling. The most efficient pedestrian air-temperature moderation will be observed in 2014 as well (0.52 K of cooling). The highest daytime pedestrian radiant relief will correspond to 2021, with MRT drop by 1.65 °C. Midnight MRT retention will favor 2014, since both high-rise forms raise MRT.

These results make the judgment about the green roof or high-rise form impossible. However, intermediate forms may pose considerable risks for pedestrian exposure. 2018 shows reduced cooling, restricted sky view, and RIB value equal to 0.51 °C. It raises midnight MRT by 0.65 °C but fails to provide daytime relief. Therefore, the temporary cooling of sidewalks becomes crucial for pedestrian protection.

5.5. Calculation Scope

The calculation involves maximum roof cooling, maximum pedestrian cooling, median sky view compression, MRT differences, and air-temperature validation values. These values explain site-specific cooling, but do not provide a detailed analysis of hourly pedestrian comfort. They reflect only maximum values without describing spatial cooling variation or time-varying shadows. Moreover, daily pedestrian exposure is not fully covered by the current data.

The limitation concerns validation weights as well. While reliable values exist for air temperatures, corresponding MRT and long-wave radiation figures are lacking for this particular study. As a result, Γ_y becomes air-temperature-based value, not physiological comfort parameter. To assess overall human comfort in air, radiant load, humidity, air velocity, activity, and attire should be included in calculations.

Such limits provide accurate interpretations of results. The Javits analysis implies the maintenance of cooling under high-rise completion and stability of the roof-to-pedestrian transfer ratio. Cooling, proportionality, radiant response, and validation values all confirm the idea that the roof continues to contribute, transfer proportionality remains steady, cooling value lowers, and MRT difference switches from unfavorable 2018 day–night ratio to 2021 day-time relief with midnight retention.

6. Conclusions

Hudson Yards high-rise construction near the Javits green roof mainly affects cooling magnitude rather than changing roof-to-street proportionality of the cooling process. The maximum cooling value at the roof level will drop from 0.75 K in 2014 to 0.64 K in 2021, while the maximum pedestrian cooling value will be reduced from 0.52 K to 0.44 K. The proportionality factor is 0.853 with morphology attenuation of 0.147.

Transfer from roofs to the streets also changes very little. For example, the transfer fraction will go from 0.693 in 2014 to 0.688 in 2021. Hence, the reduced pedestrian cooling will be caused mainly by lowered roof-level cooling values. Validation weighting of cooling also implies the maintenance of proportionality: Γ_y will be decreased from 0.650 K to 0.553 K, making up 85.1% of 2014 value.

MRT values allow answering the second part of the question. The daytime MRT reduction will rise from 0.14 °C in 2014 to 1.65 °C in 2021. However, the midnight MRT will also grow: 0.65 and 0.74 °C in 2018 and 2021, respectively. 2018 will perform worse than 2021: only 0.14 °C MRT reduction in the daytime and 0.65 °C increase at night. Therefore, high-rise completion favors daytime shading with midnight retention.

Finally, it becomes clear that the green roof continues being an important component in the roof-to-street cooling chain. The new roof form cools the roofs, while also providing minor pedestrian relief. Effective heat mitigation strategy needs to involve both roof layers, streets, and the interaction between these two zones. Thus, the numerical result is quite specific: the roof retains its capacity, proportionality is preserved, and the principal response is the separation between cooling and shading.

References

[1] Akbari, H., Cartalis, C., Kolokotsa, D., Muscio, A., Pisello, A. L., Rossi, F., ... & Zinzi, M. (2016). Local climate change and urban heat island mitigation techniques–the state of the art. *Journal of Civil Engineering and Management, 22*(1), 1-16.

[2] Alexandri, E., & Jones, P. (2008). Temperature decreases in an urban canyon due to green walls and green roofs in diverse climates. *Building and Environment, 43*(4), 480-493.

[3] Alizadehtazi, B., Stolper, J., Singh, K., & Montalto, F. A. (2024). Microclimatic implications of a large-scale green roof and high-rise redevelopment in New York City. *Building and Environment, 250*, 111113.

[4] Berardi, U. (2016). The outdoor microclimate benefits and energy saving resulting from green roofs retrofits. *Energy and Buildings, 121*, 217-230.

[5] Bowler, D. E., Buyung-Ali, L., Knight, T. M., & Pullin, A. S. (2010). Urban greening to cool towns and cities: A systematic review of the empirical evidence. *Landscape and Urban Planning, 97*(3), 147-155.

[6] Bruse, M., & Fleer, H. (1998). Simulating surface–plant–air interactions inside urban environments with a three dimensional numerical model. *Environmental Modelling & Software, 13*(3-4), 373-384.

[7] Castleton, H. F., Stovin, V., Beck, S. B., & Davison, J. B. (2010). Green roofs; building energy savings and the potential for retrofit. *Energy and Buildings, 42*(10), 1582-1591.

[8] Erell, E., Pearlmutter, D., & Williamson, T. (2011). Urban microclimate: Designing the spaces between buildings. Earthscan, London. Anglia.

[9] Getter, K. L., & Rowe, D. B. (2006). The role of extensive green roofs in sustainable development. *HortScience, 41*(5), 1276-1285.

[10] Gill, S. E., Handley, J. F., Ennos, A. R., & Pauleit, S. (2007). Adapting cities for climate change: the role of the green infrastructure. *Built Environment, 33*(1), 115-133.

[11] Johansson, E. (2006). Influence of urban geometry on outdoor thermal comfort in a hot dry climate: A study in Fez, Morocco. *Building and Environment, 41*(10), 1326-1338.

[12] Kleerekoper, L., Van Esch, M., & Salcedo, T. B. (2012). How to make a city climate-proof, addressing the urban heat island effect. *Resources, Conservation and Recycling, 64*, 30-38.

[13] Li, D., & Bou-Zeid, E. (2014). Quality and sensitivity of high-resolution numerical simulation of urban heat islands. *Environmental Research Letters, 9*(5), 055001.

[14] Oberndorfer, E., Lundholm, J., Bass, B., Coffman, R. R., Doshi, H., Dunnett, N., ... & Rowe, B. (2007). Green roofs as urban ecosystems: ecological structures, functions, and services. *BioScience, 57*(10), 823-833.

[15] Oke, T. R. (1973). City size and the urban heat island. *Atmospheric Environment (1967), 7*(8), 769-779.

[16] Oke, T. R. (1981). Canyon geometry and the nocturnal urban heat island: comparison of scale model and field observations. *Journal of Climatology, 1*(3), 237-254.

[17] Sailor, D. J. (2008). A green roof model for building energy simulation programs. *Energy and Buildings, 40*(8), 1466-1478.

[18] Santamouris, M. (2014). Cooling the cities–a review of reflective and green roof mitigation technologies to fight heat island and improve comfort in urban environments. *Solar Energy, 103*, 682-703.

[19] Santamouris, M. (2015). Analyzing the heat island magnitude and characteristics in one hundred Asian and Australian cities and regions. *Science of the Total Environment, 512*, 582-598.

[20] Salata, F., Golasi, I., de Lieto Vollaro, R., & de Lieto Vollaro, A. (2016). Urban microclimate and outdoor thermal comfort. A proper procedure to fit ENVI-met simulation outputs to experimental data. *Sustainable Cities and Society, 26*, 318-343.

[21] Stewart, I. D., & Oke, T. R. (2012). Local climate zones for urban temperature studies. *Bulletin of the American Meteorological Society, 93*(12), 1879-1900.

[22] Susca, T., Gaffin, S. R., & Dell'Osso, G. R. (2011). Positive effects of vegetation: Urban heat island and green roofs. *Environmental Pollution, 159*(8-9), 2119-2126.

[23] Taleghani, M., Kleerekoper, L., Tenpierik, M., & Van Den Dobbelsteen, A. (2015). Outdoor thermal comfort within five different urban forms in the Netherlands. *Building and Environment, 83*, 65-78.

[24] Tsoka, S., Tsikaloudaki, A., & Theodosiou, T. (2018). Analyzing the ENVI-met microclimate model's performance and assessing cool materials and urban vegetation applications–A review. *Sustainable Cities and Society, 43*, 55-76.

[25] Venhari, A. A., Tenpierik, M., & Taleghani, M. (2019). The role of sky view factor and urban street greenery in human thermal comfort and heat stress in a desert climate. *Journal of Arid Environments, 166*, 68-76.

[26] Willmott, C. J., & Wicks, D. E. (1980). An empirical method for the spatial interpolation of monthly precipitation within California. *Physical Geography, 1*(1), 59-73.

[27] Yang, J., Yu, Q., & Gong, P. (2008). Quantifying air pollution removal by green roofs in Chicago. *Atmospheric Environment, 42*(31), 7266-7273.

[28] Zhang, G., He, B. J., & Dewancker, B. J. (2020). The maintenance of prefabricated green roofs for preserving cooling performance: A field measurement in the subtropical city of Hangzhou, China. *Sustainable Cities and Society, 61*, 102314.

[29] Zinzi, M., & Agnoli, S. (2012). Cool and green roofs. An energy and comfort comparison between passive cooling and mitigation urban heat island techniques for residential buildings in the Mediterranean region. *Energy and Buildings, 55*, 66-76.